



Universiteit
Leiden
The Netherlands

Transgenic mouse models in migraine

Ven, R.C.G. van de

Citation

Ven, R. C. G. van de. (2007, November 6). *Transgenic mouse models in migraine*. Retrieved from <https://hdl.handle.net/1887/12473>

Version: Corrected Publisher's Version

License: [Licence agreement concerning inclusion of doctoral thesis in the Institutional Repository of the University of Leiden](#)

Downloaded from: <https://hdl.handle.net/1887/12473>

Note: To cite this publication please use the final published version (if applicable).

CHAPTER 5

Characterization of acetylcholine release and the compensatory contribution of non-Ca_v2.1 channels at motor nerve terminals of *leaner* Ca_v2.1-mutant mice

R.C.G. van de Ven,^{1†} S. Kaja,^{2,3§†} L.A.M. Broos,¹ R.R. Frants¹, M.D. Ferrari³, A.M.J.M. van den Maagdenberg^{1,3} and J.J. Plomp^{2,3}

[†]Authors contributed equally

¹Department of Human Genetics, ²Molecular Cell Biology - Group Neurophysiology and ³Neurology, Leiden University Medical Centre, Leiden, The Netherlands

[§]Present address: Michael Smith Laboratories, The University of British Columbia, Vancouver, Canada

Abstract

The severely ataxic and epileptic mouse *leaner* (*Ln*) carries a natural splice site mutation in *Cacna1a*, leading to a C-terminal truncation of the encoded Ca_v2.1- α_1 protein. Ca_v2.1 is a neuronal Ca²⁺ channel, mediating neurotransmitter release at many central synapses and the peripheral neuromuscular junction (NMJ). With electrophysiological analyses we demonstrate severely reduced (~50%) neurotransmitter release at *Ln* NMJs. This equals the reduction at NMJs of *Cacna1a* null-mutant (Ca_v2.1- α_1 KO) mice, which display a neurological phenotype remarkably similar to that of *Ln* mice. However, using selective Ca_v channel blocking compounds we revealed a compensatory contribution profile of non-Ca_v2.1 type channels at *Ln* NMJs that differs completely from that at Ca_v2.1- α_1 KO NMJs. Our data indicate that the residual function and presence of *Ln*-mutated Ca_v2.1 channels precludes presynaptic compensatory recruitment of Ca_v1 and Ca_v2.2 channels, and hampers that of Ca_v2.3 channels. This is the first report directly showing at single synapses the deficits and plasticity in transmitter release resulting from the *Ln* mutation of *Cacna1a*.

Abbreviations

ACh, acetylcholine; BTx, α -bungarotoxin; Ca_v2.1- α_1 KO, *Cacna1a* null-mutant mice; CNS, central nervous system; EA2, episodic ataxia type 2; EPP, endplate potential; *Ln*, *leaner*; MEPP, miniature endplate potential; NMJ, neuromuscular junction; PBS, phosphate-buffered saline

Introduction

Pore-forming subunits of neuronal voltage-activated Ca²⁺ channels are a family of membrane proteins encoded by different genes that are expressed widely throughout the nervous system.¹ The channel subtypes Ca_v2.1 (P/Q-type), Ca_v2.2 (N-type) and Ca_v2.3 (R-type) are mainly involved in mediating neurotransmitter release from central and peripheral nerve terminals. Their specialized synaptic function most likely results from their ability to localize at active zones (the presynaptic transmitter release sites), and to interact with neuroexocytotic proteins.^{2,3}

Studies in mice and rats have shown that joint contribution of Ca_v2.1, -2 and -3 channel subtypes to transmitter release is common during early development at synapses of several CNS areas (cerebral cortex, cerebellum, thalamus, hippocampus, spinal cord).^{4,5} However, during the first few postnatal weeks, the contribution of Ca_v2.2 and Ca_v2.3 is gradually lost and taken over by Ca_v2.1 channels at many types of synapses.⁴ At only a small subset (e.g. in cerebral cortex and hippocampus) release remains jointly mediated by Ca_v2.1, -2 and -3 channels.^{4,6,7} At the peripheral neuromuscular junction (NMJ), studies in rodents showed a similar developmental switch, gradually eliminating Ca_v2.2 contribution⁸, leaving Ca_v2.1 channels to control the main part (>90%) of nerve action potential-evoked release of acetylcholine (ACh) from a few weeks postnatally and onwards.⁹⁻¹²

Interestingly, the capability of joint contribution of Ca_v2.1, -2, and -3 channels to transmitter release is not permanently lost after the developmental switch, but seems to be rather generally preserved as a compensatory mechanism in case of malfunction of the original, monospecifically contributing channel. Thus, NMJs and central synapses of Ca_v2.1 *null*- and missense-mutant mice become to rely on Ca_v1, Ca_v2.2 and/or Ca_v2.3 channels¹³⁻²¹, whereas compensatory Ca_v2.1 expression occurs in Ca_v2.2 *null*-mutant neurons.²² Cultured cerebellar Purkinje cells are able of upregulating Ca_v2.3 channels after partial downregulation of Ca_v2.1 channels by antibodies.²³

Ca_v2.1 channels have been implicated in human neurological disease. Mutations in *CACNA1A*, the coding gene for the α_1 -subunit, were identified in familial hemiplegic migraine type-1, episodic ataxia type-2 (EA2), spinocerebellar ataxia type-6 and generalised epilepsy with ataxia.²⁴⁻²⁷ Furthermore, Ca_v2.1 channels at the NMJ are auto-immune targets in the neuro-immunological Lambert-Eaton myasthenic syndrome.²⁸ Compensatory expression of non-Ca_v2.1 channels may help reduce symptoms in these diseases.

A number of natural and transgenic *Cacna1a* mouse mutants, displaying a spectrum of symptoms of epilepsy and ataxia, serve as models of human Ca_v2.1 channelopathies.

Chapter 5

These include the natural mutants *leaner (Ln)*, *tottering* and *rolling Nagoya*²⁹⁻³², knock-outs^{33,34} and knock-ins.^{35,36} Characterization of the primary neuronal deficits and subsequent compensatory involvement of non-Ca_v2.1 channels in these mouse models is of particular interest. The underlying signalling pathways may harbour drug targets that might be influenced to optimize compensation.

In the present study we characterized the basic aspects of transmitter release and the compensatory contribution of non-Ca_v2.1 channels at the NMJ of natural *Ln* mutant mice. The *Ln* Ca_v2.1- α_1 protein lacks a large part of the cytoplasmic C-terminus^{29,30}, which contains important sites for interaction with other structural and functional synaptic proteins.³⁷⁻³⁹ Previously, we have shown that the mouse NMJ is a suitable model to study the synaptic effect of *CACNA1A* mutations on transmitter release.^{35,40,41} With electrophysiological measurements and selective Ca_v channel blocking compounds we here compared the ACh release characteristics of *Ln* NMJs with that of Ca_v2.1 knock-out mice (Ca_v2.1- α_1 KO), in which Ca_v2.1 channels are absent but compensated for by Ca_v2.2 and -3 channels.^{15,16} In spite of a remarkably similar neurological phenotype of these two mice strains, i.e. severe and progressive ataxia and epilepsy leading to premature death at about 3-4 weeks of age^{34,42}, we found only limited Ca_v2.3 channel contribution at *Ln* NMJs, and no Ca_v2.2 channel contribution at all. Our data indicate that the presence of truncated *Ln* Ca_v2.1- α_1 protein blocks compensatory contribution of Ca_v2.2 channels and greatly inhibits that of Ca_v2.3 channels at the NMJ.

Experimental Procedures

Mice

All animal experiments were in accordance with national legislation, the USA National Institutes of Health recommendations for the humane use of animals, and were approved by the Leiden University Animal Experiments Committee.

We generated Ca_v2.1- α_1 KO mice, essentially as described by others.³⁴ Briefly, mouse genomic DNA clones were derived from a pPAC4 library (129/SvevTACfBr strain). In the targeting vector, an *MscI-XbaI* fragment that includes part of exon 4 and intron 4 was replaced by a PGK-driven *neo* cassette, thereby disrupting the *Cacna1a* gene. ES cells (E14) were electroporated and positive clones selected for homologous recombination by Southern blot analysis, using external probes. Correctly targeted ES cells were injected into blastocysts to create chimeric animals. F1 agouti progeny were genotyped for transmission of the mutant allele and further bred with C57Bl6J mice in order to create

the transgenic Ca_v2.1- α_1 KO mouse line. Homozygous Ca_v2.1- α_1 KO mice of generation F3 were used for experiments. Successful targeting of the *Cacna1a* gene was shown by using standard molecular biological techniques similar to Jun et al. (data not shown).³⁴ The homozygous Ca_v2.1- α_1 KO mice exhibited a phenotype similar to that described by others^{33,34}, i.e. severe ataxia, epileptic seizures and premature death at 3-4 weeks of age. Homozygous *Ln* mice were obtained from heterozygous breedings. Original breeders were purchased from Jackson Laboratories (Bar Harbor, ME, USA). Wild-types served as controls (littermates if possible, otherwise age-matched non-littermates). Mice were used for experiments at age P19-21. *Ln* and Ca_v2.1- α_1 KO mice body weights were ~55% lower than wild-type (4.5 ± 0.1 , 4.5 ± 0.2 and 10.2 ± 0.6 g, respectively, $n=11-16$, $p<0.001$).

Genotyping

Genomic DNA was extracted from tail clips. Tissue was incubated in 250 μ l incubation mixture (50 mM Tris-HCl pH 9.0, 0.45% Igepal [Sigma-Aldrich], 0.4 mg/ml Prot K) at 55 °C for 4 h. After heat inactivation (10 min, 95 °C), 0.2 μ l lysate was amplified by PCR.

For genotyping of Ca_v2.1- α_1 KO mice two PCR reactions were performed. Forward primer P277 5'-CTGAGCTGATGCTGAAGCTG-3', and reverse primer P279 5'-AGACTCACGCACTTGGGATT-3' were used for detection of the wild-type allele. For the second PCR detecting the mutant allele, forward primer P354 5'-TCGGGAGCGGCGATAACCGTAAAG-3', and reverse primer P355 5'-TCCGGCCGCTTGGGTGGAGA-3' were used, both located in the *neo* cassette. PCR products of 717 bp and 204 bp, respectively, were produced.

For genotyping of *Ln* mice, forward primer P204 5'-TCGACATGCCTAACAGCCAG-3' located on exon 42, and reverse primer P205 5'-CAGTACCCATTTCTCGCATC-3' located on exon 43, produced a fragment of 151 bp. Digestion of the wild-type fragment with *Mva*I resulted in two fragments of 121 bp and 30 bp, whereas the *Ln* fragment remained uncut.

Ex vivo neuromuscular junction electrophysiology

Mice were euthanized by carbon dioxide inhalation. Phrenic nerve-hemidiaphragms were dissected and mounted in standard Ringer's medium (in mM: NaCl 116, KCl 4.5, CaCl₂ 2, MgSO₄ 1, NaH₂PO₄ 1, NaHCO₃ 23, glucose 11, pH 7.4), at room temperature (20-22 °C)

Chapter 5

and continuously bubbled with 95% O₂ / 5% CO₂. Intracellular recordings of miniature endplate potentials (MEPPs, the postsynaptic depolarizing events due to spontaneous unquantal ACh release) and endplate potentials (EPPs, the depolarization resulting from nerve action potential-evoked ACh release) were made at NMJs at 28 °C using a 10-20 MΩ glass microelectrode, filled with 3 M KCl, connected to a Geneclamp 500B (Axon Instruments/Molecular Devices, Union City, CA, USA) for amplifying and filtering (10 kHz low-pass). Signals were digitized, stored and analyzed (off-line) on a personal computer using a Digidata 1322A interface, Clampex 8.2 and Clampfit 8.2 programs (all from Axon Instruments/Molecular Devices) and routines programmed in Matlab (The MathWorks Inc., Natick, MA, USA). At least 30 MEPPs and EPPs were recorded at each NMJ, and 7-15 NMJs were sampled per experimental condition per muscle. Muscle action potentials were blocked by 3 μM of the selective muscle Na⁺ channel blocker μ-conotoxin GIIIB (Scientific Marketing Associates, Barnet, Herts, UK). In order to record EPPs, the phrenic nerve was stimulated supramaximally at 0.3 Hz and 40 Hz, using either a bipolar platinum or a suction electrode. The amplitudes of EPPs and MEPPs were normalized to -75 mV, assuming 0 mV as the reversal potential for ACh-induced current.⁴³ The normalized EPP amplitudes were corrected for non-linear summation according to⁴⁴ with an *f* value of 0.8. Quantal content, i.e. the number of ACh quanta released per nerve impulse, was calculated for each NMJ by dividing the normalized and corrected mean EPP amplitude by the normalized mean MEPP amplitude.

In order to assess the contribution of different Ca²⁺ current types on ACh release, EPPs and MEPPs were also measured in the presence of the specific Ca_v channel blockers ω-agatoxin-IVA (Ca_v2.1, 200 nM), ω-conotoxin-GVIA (Ca_v2.2, 2.5 μM), SNX-482 (Ca_v2.3, 1 μM) and nifedipine (Ca_v1, 10 μM, kept in the dark prior to the experiment). Measurements were made following a 20 min pre-incubation with toxin. All toxins were from Scientific Marketing Associates, Barnet, Herts, UK. Nifedipine (Sigma-Aldrich, Zwijndrecht, The Netherlands) was dissolved in dimethylsulfoxide to obtain a 10 mM stock solution. The final solution in Ringer's medium contained 0.1% dimethylsulfoxide. In the control condition before nifedipine incubation, electrophysiological measurements were made in Ringer's medium with 0.1% dimethylsulfoxide added. Nifedipine was pre-incubated for 1 h before starting the measurements. During pre-incubations and the electrophysiological measurements, 95% O₂ / 5% CO₂ was blown over the surface of the 2 ml medium.

α-Bungarotoxin staining and image analysis

NMJ size was determined by staining the area of ACh receptors with fluorescently labelled α-bungarotoxin (BTx), as described before.⁴¹

Muscle fibre diameter analysis

Midline muscle sections were excised from left hemidiaphragms, pinned out on blocks of silicone rubber, snap frozen in liquid nitrogen and subsequently embedded in TissueTek® (Bayer BV, Mijdrecht, The Netherlands). Transversal sections (12-18 μm) were cut on a Microm cryostat (Adamas Instruments BV, Leersum, The Netherlands), at -21° C and collected on poly-lysine coated slides, dried for 1 h at room temperature, fixed for 10 s in ice-cold acetone, stained for 10 s in 0.5% alkaline toluidine blue, dehydrated in a graded series of ethanol (50%, 70% 80%, 90%, 96%, 100%, 1 min each) and finally cleared with xylene. Sections were embedded in Entellan mounting medium (Merck, Darmstadt, Germany) and viewed under a Zeiss Axioplan light microscope (Zeiss, Jena, Germany). Digital photos were taken and fibre diameter quantified using ImageJ (National Institutes of Health, USA). Stereological considerations were taken into account by defining the actual diameter of a muscle fibre by the shortest distance measured. Ten to 15 fibres were measured per muscle.

Statistical analyses

Possible statistical differences were analysed with paired or unpaired Student's *t*-tests or analysis of variance (ANOVA) with Tukey's HSD post-hoc test, where appropriate, on grand group mean values (with *n* as the number of mice tested), calculated from the mean muscle values. Mean muscle values were calculated from the mean parameter values obtained at 6-15 NMJs per experimental condition. *p*<0.05 was considered to be significant. The data are presented as mean ± S.E.M.

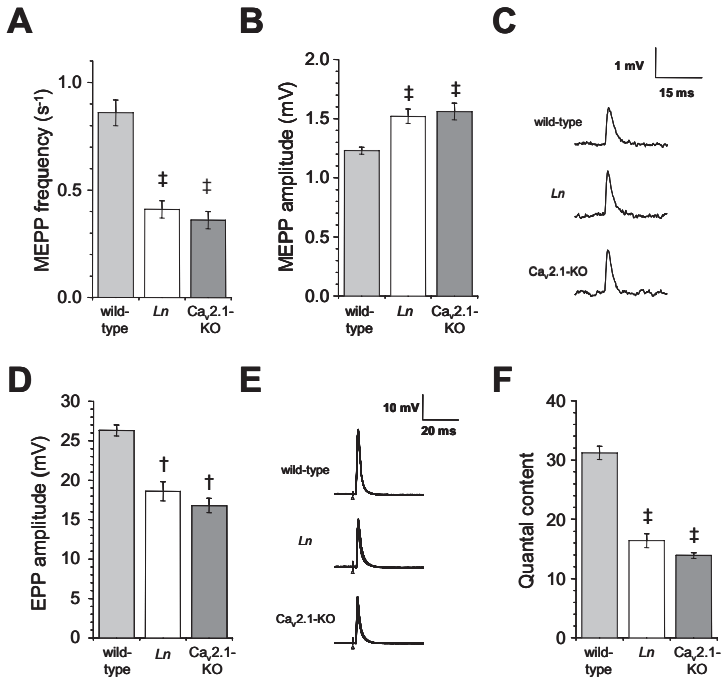


Figure 1. ACh release is reduced at the *Ln* NMJ, compared to wild-type. The extent of reduction is similar to that found at *Ca_v2.1- α_1* KO NMJs. (A) Spontaneous unquantal ACh release, measured as MEPP frequency. (B) MEPP amplitude was ~25% increased at *Ln* and *Ca_v2.1- α_1* KO NMJs. (C) Example MEPP recordings. (D) Low-rate (0.3 Hz) evoked EPP amplitude is ~35% reduced at *Ln* and *Ca_v2.1-KO* NMJs, compared to wild-type. (E) Example 0.3 Hz EPP recordings. For each genotype, 20 superimposed EPPs are shown. Triangles indicate moment of nerve stimulation. (F) The calculated quantal content was reduced by about half at both *Ln* and *Ca_v2.1- α_1* KO NMJs. † $p < 0.01$, ‡ $p < 0.001$, different from wild-type.

Results

*Similar reduction of ACh release at NMJs of *Ln* and *Ca_v2.1-KO* mice*

We first studied the basic NMJ electrophysiology of *Ln* and our newly generated *Ca_v2.1- α_1* KO mice. Spontaneous unquantal ACh release from motor nerve terminals, measured as MEPP frequency, was decreased by ~50% in both *Ln* and *Ca_v2.1- α_1* KO mice, compared with wild-type (0.41 ± 0.04 and 0.34 ± 0.04 vs. 0.86 ± 0.06 s⁻¹, respectively, $n=13-18$ mice, $p < 0.001$; Fig. 1A). MEPP amplitude, i.e. the size of the postsynaptic response to unquantal ACh release, was ~20% higher at both *Ln* and *Ca_v2.1-KO* NMJs ($n=13-18$, $p < 0.001$, Fig. 1B, C).

Nerve stimulation-evoked ACh release upon low-rate (0.3 Hz) stimulation of the phrenic nerve was greatly reduced at both *Ln* and Ca_v2.1- α_1 KO NMJs, as judged from the EPP amplitudes that were only ~65% of wild-type (n=13-18 mice, $p < 0.001$, Fig. 1D, E). The quantal contents, calculated from EPP and MEPP amplitudes, were ~50% reduced (31.2 ± 1.1 , 16.4 ± 1.2 and 13.9 ± 0.5 at wild-type, *Ln* and Ca_v2.1- α_1 KO NMJs, respectively, n=13-18 mice, $p < 0.001$, Fig. 1F).

We also studied the short-term depression of ACh release during high-rate (40 Hz) nerve stimulation, which approximates the physiological firing rate of rodent motor nerves.⁴⁵ Both *Ln* and Ca_v2.1- α_1 KO showed a significantly more pronounced rundown of EPP amplitudes than that seen in wild-type (Fig. 2A, B). The average amplitude of the 21st-35th EPP (e.g. the plateau phase) of the trains, expressed as percentage of the amplitude of the first EPP, was 68 ± 1 , 65 ± 2 and $77 \pm 1\%$ at *Ln*, Ca_v2.1- α_1 KO and wild-type NMJs, respectively (n=6 mice, $p < 0.001$, Fig. 2C). During the plateau phase, EPP amplitudes at *Ln* and Ca_v2.1- α_1 KO NMJs fluctuated much more than at wild-types. The coefficient of variance of the 21st-35th EPP amplitude was 0.06 ± 0.01 , 0.19 ± 0.02 and 0.25 ± 0.02 at wild-type, *Ln* and Ca_v2.1-KO NMJs, respectively (n=6 mice, $p < 0.001$, Fig. 2D).

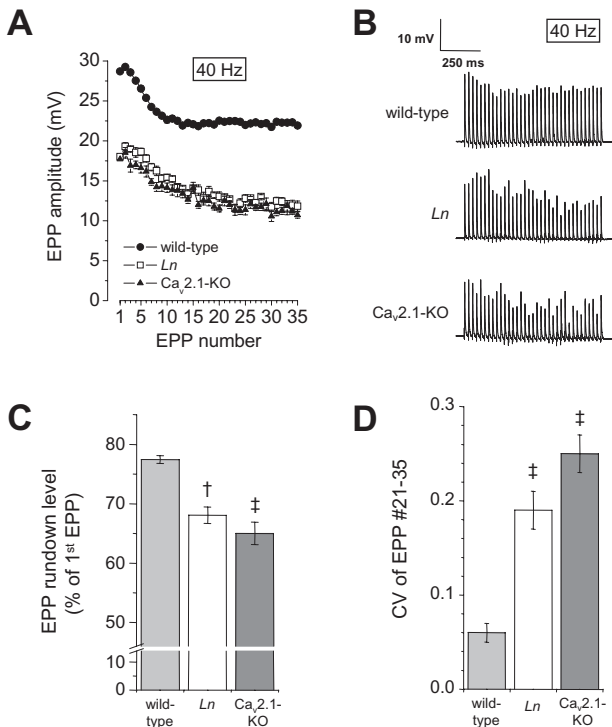


Figure 2. Increased rundown of EPP amplitude during high-rate (40 Hz) nerve stimulation at both *Ln* and Ca_v2.1- α_1 KO NMJs. (A) Averaged EPP amplitude rundown profiles. (B) Representative 1 s recording traces of 40 Hz EPP trains. (C) Normalized EPP amplitude rundown level (mean EPP amplitude of the 21st-35th EPP, expressed as percentage of the first EPP) is more pronounced at both *Ln* and Ca_v2.1- α_1 KO NMJs. (D) *Ln* and Ca_v2.1- α_1 KO NMJs display larger coefficient of variance (CV), compared to wild-type, of the amplitude of EPP number 21-35 of a 40 Hz train. † $p < 0.01$, ‡ $p < 0.001$, different from wild-type.

Compensatory contribution of non-Ca_v2.1 channels at *Ln* and Ca_v2.1- α_1 KO NMJs

In wild-type mice, nerve stimulation-evoked neurotransmitter release at the NMJ is dependent almost exclusively on Ca_v2.1 channels.^{9,12,35,46} It has been reported that the Ca_v2.1 deficiency at NMJs of Ca_v2.1- α_1 KO mice is compensated for by Ca_v2.2 and -3 channels.¹⁵ Here we studied such compensatory contribution of non-Ca_v2.1 channels at *Ln* NMJs, using selective Ca_v blocking compounds, and compared it with NMJs of the Ca_v2.1- α_1 KO mice generated in our laboratory and wild-type mice.

At wild-type NMJs, ω -agatoxin-IVA (200 nM) reduced 0.3 Hz nerve stimulation-evoked ACh release by 96.2 \pm 0.7% (quantal content before and after application of toxin was 31.3 \pm 1.6 and 1.2 \pm 0.2, n=4 mice, *p*<0.001, Fig. 3A), confirming the almost complete dependence on Ca_v2.1 channels. The quantal content at wild-type NMJs did not change upon incubation with either ω -conotoxin-GVIA (2.5 μ M), SNX-482 (1 μ M) or nifedipine (10 μ M), indicating that Ca_v2.2, Ca_v2.3 and Ca_v1 channels do not contribute to ACh release at the wild-type NMJ.

At NMJs of our Ca_v2.1- α_1 KO mice, as expected, evoked ACh release was ω -agatoxin-

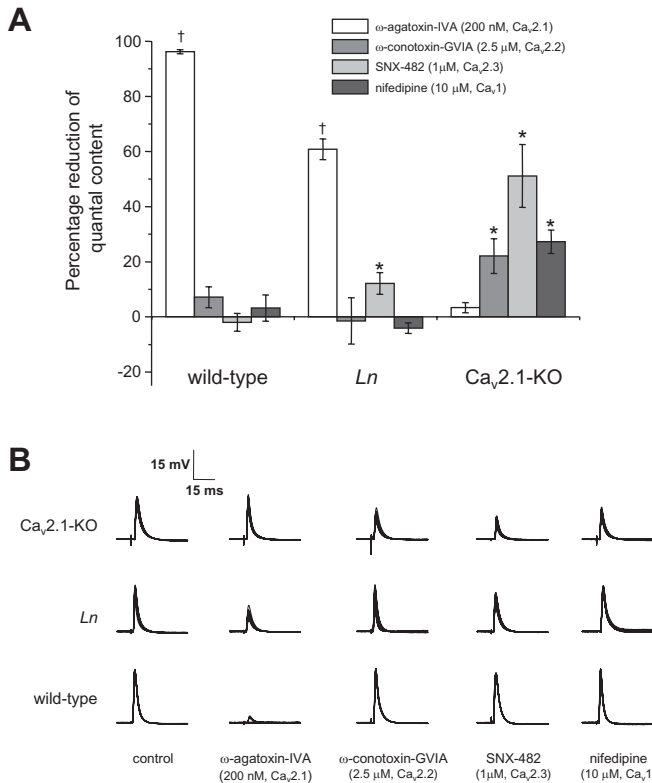


Figure 3. Differential effects of blockers of specific Ca_v channels on 0.3 Hz evoked ACh release at the wild-type, *Ln* and Ca_v2.1- α_1 KO NMJ. **(A)** Effect on quantal content. Values represent the mean percentage of reduction of quantal content induced by the specific compound. n=3-7 mice per condition, 6-15 NMJs measured per muscle. **p*<0.05, †*p*<0.01, different from control the condition before application of the blocking compound. **(B)** Representative EPP recording traces. Ten superimposed EPPs are drawn per condition and genotype.

IVA-insensitive, confirming the absence of Ca_v2.1 channels (Fig. 3). The quantal content was 14.5 ± 0.3 and 14.0 ± 0.5 before and after application of the toxin, respectively (n=3 mice, $p=0.21$). However, Ca_v2.2 blocker ω -conotoxin-GVIA reduced the quantal content by $22.1 \pm 6.3\%$ (13.3 ± 1.2 and 10.2 ± 0.9 before and after application of toxin, respectively, n=6 mice, $p<0.05$, Fig. 3). The Ca_v2.3 blocker SNX-482 reduced the quantal content (by $\sim 50\%$, from 15.2 ± 0.7 to 7.6 ± 2.0 , n=4, $p<0.05$, Fig. 3), as did the Ca_v1 channel blocker nifedipine (by $\sim 27\%$, from 13.5 ± 0.7 to 9.8 ± 0.8 , n=4 mice, $p<0.01$, Fig. 3). These results show that there is joint contribution of Ca_v1, Ca_v2.2 and Ca_v2.3 channels in evoked ACh release, compensating for the deficiency of Ca_v2.1 channels at Ca_v2.1- α_1 KO NMJs.

At the *Ln* NMJ, however, a very different picture emerged. ω -Agatoxin-IVA reduced the evoked ACh release by $\sim 60\%$ (quantal content decreased from 15.9 ± 1.2 to 6.1 ± 0.4 , n=4 mice, $p<0.001$, Fig. 3). A small proportion ($\sim 13\%$) of evoked ACh release at *Ln* NMJs was SNX-482 sensitive (the quantal content decreased from 15.7 ± 1.1 to 13.7 ± 0.7 , n=6 mice, $p<0.05$, Fig. 3). ω -Conotoxin-GVIA or nifedipine did not change quantal content (Fig. 3). These data show compensatory contribution of Ca_v2.3 channels at *Ln* NMJs and, furthermore, that $\sim 25\%$ of the evoked ACh release is not blocked by the compounds used, suggesting compensatory contribution of another, unknown Ca_v channel. It might be speculated that the *Ln* mutation renders the Ca_v2.1 channel less sensitive to ω -agatoxin-IVA and that 200 nM of the toxin is a sub-optimal concentration that only blocks part of the Ca_v2.1 channels. Therefore, we tested the effect of 600 nM of the toxin in one *Ln* muscle. The quantal content decreased by $\sim 67\%$ (from 16.1 ± 0.9 to 5.3 ± 0.5 , 10 NMJs sampled before and during toxin incubation, $p<0.001$). This reduction is similar to that induced by 200 nM ω -agatoxin-IVA, indicating that *Ln*-Ca_v2.1 channels retain normal ω -agatoxin-IVA sensitivity.

Spontaneous unquantal ACh release at wild-type NMJs, measured as MEPP frequency, was reduced by 200 nM ω -agatoxin-IVA, as published before by us and others^{35,40,41,46}, by $72.4 \pm 2.2\%$, from 0.95 ± 0.07 to 0.26 ± 0.01 , n=4 mice ($p<0.01$). All other Ca_v blockers tested had no effect on wild-type MEPP frequency (Table 1). At Ca_v2.1- α_1 KO NMJs, only SNX-482 (1 μ M) reduced MEPP frequency, by $39.1 \pm 8.7\%$, from 0.42 ± 0.07 to 0.25 ± 0.05 s⁻¹ (n=4 mice, $p<0.05$, Table 1), while all other blockers did not change this parameter. At *Ln* NMJs, ω -agatoxin-IVA, but not the other blockers, reduced MEPP frequency by $\sim 30\%$ (from 0.53 ± 0.05 to 0.38 ± 0.06 , n=4 mice, $p<0.05$, Table 1). Thus, *Ln*-Ca_v2.1 channels still contribute to some extent to spontaneous ACh release and there is no compensatory contribution by Ca_v2.2, Ca_v2.3 or Ca_v1 channels. The abolished Ca_v2.1 contribution at Ca_v2.1- α_1 KO NMJs is partly compensated for by Ca_v2.3 channels.

Table 1. Effect of specific Ca_v blockers on spontaneous unquantal ACh release.

compound - (selectivity)	wild-type	<i>Ln</i>	$\text{Ca}_v2.1\text{-KO}$
ω -agatoxin-IVA, 200 nM - ($\text{Ca}_v2.1$)	$-72.4 \pm 2.2\% \dagger$	$-27.0 \pm 8.0\%^*$	$3.5 \pm 13.4\%$
ω -conotoxin-GVIA, 2.5 μM - ($\text{Ca}_v2.2$)	$-7.0 \pm 7.6\%$	$11.3 \pm 19.8\%$	$8.6 \pm 3.4\%$
SNX-482, 1 μM - ($\text{Ca}_v2.3$)	$2.4 \pm 5.2\%$	$-9.1 \pm 7.2\%$	$-39.1 \pm 8.7\%^*$
nifedipine, 10 μM - (Ca_v1)	$13.1 \pm 11.7\%$	$-8.0 \pm 13.5\%$	$-12.4 \pm 16.2\%$

Comparison of the effect of various blockers of Ca_v channels on spontaneous ACh release, measured as MEPP frequency, at wild-type, *Ln* and $\text{Ca}_v2.1\text{-}\alpha_1$ KO NMJs. Data is expressed as the percentage change induced by the compound of the mean MEPP frequency measured in the control period before compound application. $n=3\text{-}6$ mice per condition, 6-15 NMJs measured per muscle. $^*p<0.05$, $\dagger p<0.01$, different from the condition before application of the blocking compound.

Table 2. Reduced NMJ size and muscle fibre diameter in *Ln* and $\text{Ca}_v2.1\text{-KO}$ diaphragm.

Size parameter	wild-type	<i>Ln</i>	$\text{Ca}_v2.1\text{-KO}$
NMJ area (μm^2)	328.7 ± 11.5	$243.0 \pm 13.6 \dagger (-26\%)$	$212.2 \pm 18.3 \ddagger (-35\%)$
NMJ perimeter (μm)	74.4 ± 2.4	$66.3 \pm 2.1^* (-11\%)$	$64.1 \pm 0.7 \dagger (-14\%)$
NMJ length (μm)	28.3 ± 1.4	27.0 ± 0.8	25.7 ± 0.6
NMJ width (μm)	14.4 ± 0.4	$12.5 \pm 0.4^* (-13\%)$	$11.8 \pm 0.4 \dagger (-18\%)$
Fibre diameter (μm)	18.1 ± 2.3	$10.9 \pm 0.9^* (-40\%)$	$8.7 \pm 0.9^* (-52\%)$

Quantification of NMJ size (fluorescent-BTx staining) and muscle fibre diameter (toluidine blue staining) in wild-type, *Ln* and $\text{Ca}_v2.1\text{-}\alpha_1$ KO diaphragm muscle. $n=5$ mice per genotype, 10-20 NMJs/fibres measured per muscle. $^*p<0.05$, $\dagger p<0.01$, $\ddagger p<0.001$, different from wild-type, percentage change indicated in parentheses.

Reduction of NMJ size and muscle fibre diameter at both *Ln* and $\text{Ca}_v2.1\text{-KO}$ mice

ACh release at the NMJ is roughly correlated with NMJ size^{47,48}, and reduced NMJ size has indeed been reported for $\text{Ca}_v2.1\text{-}\alpha_1$ KO mice.¹⁵ In view of this, the observed reduced ACh release at NMJs of *Ln* mice may be associated with a NMJ size reduction as well. We quantified the size of postsynaptic ACh receptor clusters as identified by Alexa Fluor 488 conjugated BTx. The area, width and perimeter of the stained surface at *Ln* NMJs was reduced by 11-26%, compared to wild-type ($n=5$ mice, 15 NMJs per muscle, Table 2). $\text{Ca}_v2.1\text{-}\alpha_1$ KO NMJs showed similar reductions (Table 2). We also quantified muscle fibre diameter. Measurement of toluidine blue stained transversal freeze sections revealed ~45% reduced fibre diameter, compared to wild-type, in both *Ln* and $\text{Ca}_v2.1\text{-}\alpha_1$ KO diaphragms ($n=3$ mice, 15 fibres per muscle, $p<0.01$, Table 2).

Discussion

We characterized the basic properties of ACh release and the compensatory contributions of non-Ca_v2.1 channels at NMJs of the natural *Cacnala* mutant mouse *Ln*, and compared it with Ca_v2.1- α_1 KO NMJs. Despite similar neurological symptoms (severe ataxia and epilepsy) and a similar basic NMJ functional phenotype (~50% reduced ACh release, compared to wild-type), a completely different compensatory profile of non-Ca_v2.1 channel contribution was revealed between the two mutants. This is the first report showing the consequences of the *Ln Cacnala* mutation on neurotransmitter release *directly* measured at a single synapse. The reduction of ACh release at the *Ln* NMJ and the compensatory Ca_v channel profile are discussed below.

Reduced nerve stimulation-evoked neurotransmitter release at the Ln NMJ

The *Ln* phenotype is caused by a splice site mutation, giving rise to two novel Ca_v2.1 *Cacnala* transcripts ('long' and 'short') with truncated cytoplasmic C-terminals.^{29,30} Although histology indicated normal mRNA and Ca_v2.1- α_1 protein level in the *Ln* cerebellum⁴⁹, electrophysiological studies showed reduced Ca²⁺ current density.^{31,50,51} This implicates functional abnormalities of the *Ln*-mutated Ca_v2.1 channel. Indeed, ~70% reduced open-probability and a small positive shift of activation- and inactivation voltage were shown.^{50,51} Thus, our observation of ~50% reduced quantal content at the *Ln* NMJ can be explained by reduced presynaptic Ca²⁺ influx during a nerve action potential, following from impaired function of individual *Ln*-mutated Ca_v2.1 channels. It is unclear whether reduced Ca_v2.1 channel *number* also contributes. The compensatory involvement of Ca_v2.3 channels suggests that this may indeed be the case (see below).

Besides a lower initial ACh release, *Ln* NMJs showed a more pronounced EPP amplitude rundown than wild-type NMJs during 40 Hz repetitive stimulation. Normal rundown at wild-type NMJs (by about ~23%) is likely determined by multiple factors: Ca_v2.1 channel inactivation, its recovery, and replenishment of releasable transmitter vesicles. Rundown normally becomes less pronounced (or even reverses in run-up) at low quantal content, e.g. upon partial inhibition of Ca_v2.1 channels with submaximal concentrations of ω -agatoxin-IVA (S. Kaja, unpublished observation) or reduction of channels by anti-Ca_v2.1 antibodies.⁵² The less pronounced rundown in these cases most likely results from the Ca²⁺ influx level being within a critical range (not saturating the Ca²⁺ sensor of the release mechanism), in combination with accumulation of cytoplasmic Ca²⁺ during the repetitive stimulation. Our observation of *more* EPP rundown at the *Ln* NMJ, despite lowered quantal content, therefore indicates that *Ln*-Ca_v2.1 channels

possess abnormal biophysical properties, rather than just being reduced in number. Although it is as yet unclear how the larger coefficient of variance of *Ln* EPP amplitude during 40 Hz trains is caused, this effect points to altered channel characteristics rather than to impaired replenishment of synaptic vesicles for release.

Like at *Ln* NMJs, we found ~50% reduction of quantal content at NMJs from $\text{Ca}_v2.1\text{-}\alpha_1$ KO mice, compared to wild-type, confirming the findings in an earlier generated other $\text{Ca}_v2.1\text{-}\alpha_1$ KO mouse.¹⁵

We observed a reduced (~40-50%) muscle fibre diameter at *Ln* and $\text{Ca}_v2.1\text{-}\alpha_1$ KO diaphragms, compared to wild-type, most likely resulting from growth retardation (*Ln* and $\text{Ca}_v2.1\text{-}\alpha_1$ KO body weight was ~55% lower than wild-type). In normal muscle, fibre diameter is known to be inversely related with electrical input resistance, which, in turn, dictates MEPP amplitude.⁵³ Furthermore, fibre diameter is positively correlated with NMJ size and ACh release level.^{47,54} Therefore, the reduced muscle fibre diameter may explain the somewhat increased MEPP amplitude, compared to wild-type, measured at *Ln* and $\text{Ca}_v2.1\text{-}\alpha_1$ KO NMJs. In agreement with the smaller fibre diameter, we observed ~30% reduced NMJ area at *Ln* and $\text{Ca}_v2.1\text{-}\alpha_1$ KO NMJs, compared to wild-type. Hence, some of the reduction of ACh release may result from smaller motor nerve terminals.

An about 50% reduced nerve stimulation-evoked ACh release, accompanied by reduced synapse size, has also been shown at NMJs in muscle biopsies from two EA2 patients heterozygous for *CACNA1A* mutations leading to a severely truncated and non-functional $\text{Ca}_v2.1$ protein.^{55,56} Compensatory contribution of $\text{Ca}_v2.2$, but not Ca_v1 channels, was found. The similarities between EA2 and *Ln* and/or $\text{Ca}_v2.1\text{-}\alpha_1$ KO NMJs suggest that these mice might serve as a model for human EA2, as hypothesized earlier on the basis of CNS studies in these mice for review, see⁵⁷.

Spontaneous ACh release is reduced at Ln NMJs

Spontaneous unquantal ACh release at the wild-type mouse NMJ is for a large part dependent on $\text{Ca}_v2.1$ channels, as demonstrated by the 50-75% inhibition of MEPP frequency by 200 nM ω -agatoxin-IVA (this study).^{35,40,46} We previously hypothesized opening of normal $\text{Ca}_v2.1$ channels already at resting membrane potential.⁴⁰ The ~50% reduced MEPP frequency at *Ln* NMJs, compared to wild-type, indicates reduced presynaptic Ca^{2+} influx at the resting motor nerve terminal, presumably due to impaired *Ln*- $\text{Ca}_v2.1$ channel function, as elaborated above. The observed ~50% reduction of MEPP frequency at $\text{Ca}_v2.1\text{-}\alpha_1$ KO NMJs confirms the reduction reported in the $\text{Ca}_v2.1$ -KO mouse generated by Urbano et al (2003). About 40% of the spontaneous ACh release at $\text{Ca}_v2.1\text{-}\alpha_1$ KO NMJs is mediated by $\text{Ca}_v2.3$ channels, as indicated by the SNX-482

experiments. The insensitivity of MEPP frequency to ω -conotoxin-GVIA and nifedipine, in contrast to the sensitivity of evoked ACh release (see above), indicates that the Ca²⁺ influx at resting potential through Ca_v1 and Ca_v2.2 channels is too small to trigger release. This may be explained by these channels being localized more distantly from release sites than Ca_v2.3 channels¹⁵, or opening less at resting membrane potential.

Differential compensatory contribution of non-Ca_v2.1 channels at *Ln* and Ca_v2.1-KO NMJs

Despite the phenotypic and NMJ function similarities between *Ln* and Ca_v2.1- α_1 KO mice, we found an intriguingly distinct profile of compensatory contribution of non-Ca_v2.1 channel to evoked ACh release: at *Ln* NMJs there was ~10% contribution of Ca_v2.3 channels and ~25% of an unidentifiable Ca_v channel, while at Ca_v2.1- α_1 KO NMJs there was contribution of Ca_v1 (~20%), Ca_v2.2 (~25%) and Ca_v2.3 (~50%) channels. Apparently, compensatory expression of these channel types is less needed at the *Ln* NMJ. These different profiles allow for some speculation on the mechanisms underlying recruitment of compensatory Ca_v channels. Our data suggest that the remaining *Ln*-Ca_v2.1 channels preclude compensatory contribution of Ca_v2.2 channels completely, and that of Ca_v2.3 channels partly. It has been hypothesized that transmitter release sites have type-specific 'slots' that are preferentially filled with Ca_v2.1 channels, but in their absence become occupied by Ca_v2.3 channels.^{13,15} Since *Ln*-Ca_v2.1 channels still contribute to ACh release, the carboxy-terminal tail is apparently not absolutely required for 'slot' occupation, despite harbouring an active zone interaction site.³⁷ Carboxy-terminal redundancy in subcellular Ca_v2.1 localization has also been suggested in recent expression studies.⁵⁸ The cytoplasmic synaptic protein interaction (synprint) site, remaining intact in *Ln*-Ca_v2.1 channels, may be of importance. It binds exocytotic machinery components for review, see³, and may thereby allow (*Ln*-)Ca_v2.1 channels to localize at active zones. Although Ca_v2.2 channels possess a synprint site, they apparently do not occupy 'slots' at *Ln* as well as wild-type NMJs. Possibly, Ca_v2.2 channels are inhibited through Ca_v2.1 channel-mediated Ca²⁺ influx stimulating syntaxin-1A expression⁵⁹, subsequently promoting G-protein-dependent inhibition of Ca_v2.2 channels.⁶⁰ Such a mechanism may also explain compensatory recruitment of Ca_v2.2 channels at the Ca_v2.1-KO NMJ. However, Ca_v2.3 channels do not have a synprint site but are compensatorily contributing to ACh release at *Ln* as well as Ca_v2.1- α_1 KO NMJs. Thus, there must be other mechanisms as well. For instance, the β_4 accessory subunit can affect channel recruitment by combined binding to multiple sites on the Ca_v2 subunit, including one at the C-terminus.⁶¹ Such binding uninhibits a Ca_v2.1 protein retention signal to the endoplasmic reticulum exerted by the

Chapter 5

I-II loop.^{61,62} Since the C-terminal is absent in *Ln*-Ca_v2.1 protein, reduced β₄-binding may cause some retention of Ca_v2.1 subunits and in this way allow Ca_v2.3 channel incorporation.

About 25% of the evoked ACh release at *Ln* NMJs was insensitive to compounds blocking either Ca_v1, Ca_v2.1, Ca_v2.2 or Ca_v2.3 channels. Possibly, this remainder derives from Ca²⁺ influx through SNX-482 insensitive Ca_v2.3 channel isoforms⁶³⁻⁶⁵ or through Ca_v3 (T-type) channels, although the latter channel is less likely because it lacks synaptic interaction sites and has not yet been associated with neurotransmitter release.¹

Our finding of compensatory Ca_v1 involvement in evoked ACh release at NMJs of Ca_v2.1-α₁ KO mice contrasts the study of Urbano et al (2003), where no such contribution was identified using 10 μM nimodipine, despite immunohistochemical demonstration of Ca_v1.3 (α_{1D}) channel presence.¹⁶ Subtle genetic background differences between our two Ca_v2.1-KO mouse lines may be one factor accounting for this differential profile. Furthermore, although age of experimental mice was not explicitly noted in the paper of Urbano and colleagues¹⁵, lower quantal content and MEPP frequency, larger MEPP amplitude and smaller NMJ size of their wild-type mice, compared to wild-type values in the present study, suggest that experimental groups were younger than the ~20 days of age at which we performed experiments. The possibility cannot be excluded that compensatory Ca_v1 contribution only first develops during the third postnatal week.

Some cross-activity on non-Ca_v2.3 channels has been reported for SNX-482, although the emerging picture is very inconsistent.⁶⁶⁻⁶⁹ If true, some degree of distortion might be present in our Ca_v subtype-characterizations. However, the reducing effect of 1 μM SNX-482 on quantal content at Ca_v2.1-α₁ KO NMJs after treatment with 2.5 μM ω-conotoxin-IVA is similar to the effect of SNX-482 alone (S. Kaja, unpublished data). This excludes Ca_v2.2 channel block by SNX-482 at the mouse NMJ. Most studies characterizing SNX-482 specificity showed a lack of effect of the toxin on Ca_v1 channels, and we assume this also holds for the NMJ. Only Bourinet et al. (2001) described incomplete and reversible block of transfected Ca_v1 channels by 1.5 μM SNX-482. Several studies demonstrated that SNX-482 (up to 1 μM) had no effect on Ca_v2.1 channels (this study).^{15,70,71} It is surprising, therefore, that Arroyo et al. (2003) suggested efficient block of Ca_v2.1 channels by 0.3 μM SNX-482.

Further insights into the exact mechanism of compensatory expression of Ca_v channels at synapses will be instrumental in understanding the cell type-specific effects of *Cacna1a* mutations.

Acknowledgements

We thank Dr. J.N. Noordermeer (Dept. of Molecular Cell Biology) for use of the fluorescence microscope and M.G.M. Deenen and H. Choufoer (Dept. of Neurosurgery) for help with muscle fibre histology. This work was supported by grants from the Prinses Beatrix Fonds (#MAR01-0105, to JJP), the Hersenstichting Nederland (#9F01(2).24, to JJP), KNAW van Leersumfonds (to JJP), the Netherlands Organisation for Scientific Research, NWO (an EMBL travel bursary to SK, and a VICI grant 918.56.602, to MDF), a 6th Framework specific targeted research project EUROHEAD (LSHM-CT-2004-504837, to MDF) and the Centre for Medical Systems Biology (CMSB) established by the Netherlands Genomics Initiative/Netherlands Organisation for Scientific Research (NGI/NWO).

A small part of the present results has been presented in preliminary form at the Xth International Conference on Myasthenia Gravis and Related Disorders (2002, Key Biscayne, USA), and has been published in short in the conference proceedings.⁷²

References

1. Catterall, W.A. Structure and regulation of voltage-gated Ca₂₊ channels. *Annu. Rev. Cell Dev. Biol.* **16**, 521-555 (2000).
2. Jones, S.W. Calcium channels: unanswered questions. *J. Bioenerg. Biomembr.* **35**, 461-475 (2003).
3. Spafford, J.D. & Zamponi, G.W. Functional interactions between presynaptic calcium channels and the neurotransmitter release machinery. *Curr. Opin. Neurobiol.* **13**, 308-314 (2003).
4. Iwasaki, S., Momiyama, A., Uchitel, O.D. & Takahashi, T. Developmental changes in calcium channel types mediating central synaptic transmission. *J. Neurosci.* **20**, 59-65 (2000).
5. Kamp, M.A. *et al.* Presynaptic 'Ca_v2.3-containing' E-type Ca channels share dual roles during neurotransmitter release. *Eur. J. Neurosci.* **21**, 1617-1625 (2005).
6. Luebke, J.I., Dunlap, K. & Turner, T.J. Multiple calcium channel types control glutamatergic synaptic transmission in the hippocampus. *Neuron* **11**, 895-902 (1993).
7. Wheeler, D.B., Randall, A. & Tsien, R.W. Roles of N-type and Q-type Ca₂₊ channels in supporting hippocampal synaptic transmission. *Science* **264**, 107-111 (1994).
8. Urbano, F.J., Rosato-Siri, M.D. & Uchitel, O.D. Calcium channels involved in neurotransmitter release at adult, neonatal and P/Q-type deficient neuromuscular junctions (Review). *Mol. Membr. Biol.* **19**, 293-300 (2002).
9. Bowersox, S.S. *et al.* Differential blockade of voltage-sensitive calcium channels at the mouse neuromuscular junction by novel omega-conopeptides and omega-agatoxin-IVA. *J. Pharmacol. Exp. Ther.* **273**, 248-256 (1995).
10. Hong, S.J. & Chang, C.C. Inhibition of acetylcholine release from mouse motor nerve by a P-type calcium channel blocker, omega-agatoxin IVA. *J. Physiol.* **482**, 283-290 (1995).
11. Lin, M.J. & Lin-Shiau, S.Y. Multiple types of Ca₂₊ channels in mouse motor nerve terminals. *Eur. J. Neurosci.* **9**, 817-823 (1997).

Chapter 5

12. Uchitel,O.D. *et al.* P-type voltage-dependent calcium channel mediates presynaptic calcium influx and transmitter release in mammalian synapses. *Proc. Natl. Acad. Sci. U. S. A* **89**, 3330-3333 (1992).
13. Cao,Y.Q. *et al.* Presynaptic Ca²⁺ channels compete for channel type-preferring slots in altered neurotransmission arising from Ca²⁺ channelopathy. *Neuron* **43**, 387-400 (2004).
14. Leenders,A.G. *et al.* Neurotransmitter release from tottering mice nerve terminals with reduced expression of mutated P- and Q-type Ca²⁺-channels. *Eur. J. Neurosci.* **15**, 13-18 (2002).
15. Urbano,F.J. *et al.* Altered properties of quantal neurotransmitter release at endplates of mice lacking P/Q-type Ca²⁺ channels. *Proc. Natl. Acad. Sci. U. S. A* **100**, 3491-3496 (2003).
16. Pagani,R. *et al.* Differential expression of alpha(1) and beta subunits of voltage dependent Ca(2+) channel at the neuromuscular junction of normal and p/q Ca(2+) channel knockout mouse. *Neuroscience* **123**, 75-85 (2004).
17. Qian,J. & Noebels,J.L. Presynaptic Ca(2+) influx at a mouse central synapse with Ca(2+) channel subunit mutations. *J. Neurosci.* **20**, 163-170 (2000).
18. Inchauspe,C.G., Martini,F.J., Forsythe,I.D. & Uchitel,O.D. Functional compensation of P/Q by N-type channels blocks short-term plasticity at the calyx of held presynaptic terminal. *J. Neurosci* **24**, 10379-10383 (2004).
19. Ishikawa,T., Kaneko,M., Shin,H.S. & Takahashi,T. Presynaptic N-type and P/Q-type Ca²⁺ channels mediating synaptic transmission at the calyx of Held of mice. *J. Physiol* **568**, 199-209 (2005).
20. Kaja,S. *et al.* Compensatory contribution of cav2.3 channels to acetylcholine release at the neuromuscular junction of tottering mice. *J. Neurophysiol.* **95**, 2698-2704 (2006).
21. Etheredge,J.A., Murchison,D., Abbott,L.C. & Griffith,W.H. Functional compensation by other voltage-gated Ca(2+) channels in mouse basal forebrain neurons with Ca(V)2.1 mutations. *Brain Res.* **Article in press**, (2005).
22. Takahashi,E., Ino,M., Miyamoto,N. & Nagasu,T. Expression analysis of P/Q-type Ca²⁺ channel alpha 1A subunit mRNA in olfactory mitral cell in N-type Ca²⁺ channel alpha 1B subunit gene-deficient mice. *Neurosci. Lett.* **359**, 37-40 (2004).
23. Pinto,A. *et al.* Human autoantibodies specific for the alpha1A calcium channel subunit reduce both P-type and Q-type calcium currents in cerebellar neurons. *Proc. Natl. Acad. Sci. U. S. A* **95**, 8328-8333 (1998).
24. Jouvenceau,A. *et al.* Human epilepsy associated with dysfunction of the brain P/Q-type calcium channel. *Lancet* **358**, 801-807 (2001).
25. Ophoff,R.A. *et al.* Familial hemiplegic migraine and episodic ataxia type-2 are caused by mutations in the Ca²⁺ channel gene CACNL1A4. *Cell* **87**, 543-552 (1996).
26. Zhuchenko,O. *et al.* Autosomal dominant cerebellar ataxia (SCA6) associated with small polyglutamine expansions in the alpha 1A-voltage-dependent calcium channel. *Nat. Genet.* **15**, 62-69 (1997).
27. Imbrici,P. *et al.* Dysfunction of the brain calcium channel CaV2.1 in absence epilepsy and episodic ataxia. *Brain* **127**, 2682-2692 (2004).
28. Lennon,V.A. *et al.* Calcium-channel antibodies in the Lambert-Eaton syndrome and other paraneoplastic syndromes. *N. Engl. J. Med.* **332**, 1467-1474 (1995).
29. Doyle,J., Ren,X., Lennon,G. & Stubbs,L. Mutations in the Cacn1Ia4 calcium channel gene are associated with seizures, cerebellar degeneration, and ataxia in tottering and leaner mutant mice. *Mamm. Genome* **8**, 113-120 (1997).
30. Fletcher,C.F. *et al.* Absence epilepsy in tottering mutant mice is associated with calcium channel defects. *Cell* **87**, 607-617 (1996).
31. Lorenzon,N.M., Lutz,C.M., Frankel,W.N. & Beam,K.G. Altered calcium channel currents in Purkinje cells of the neurological mutant mouse leaner. *J. Neurosci.* **18**, 4482-4489 (1998).
32. Mori,Y. *et al.* Reduced voltage sensitivity of activation of P/Q-type Ca²⁺ channels is associated with the ataxic mouse mutation rolling Nagoya (tg(rol)). *J. Neurosci.* **20**, 5654-5662 (2000).
33. Fletcher,C.F. *et al.* Dystonia and cerebellar atrophy in Cacna1a null mice lacking P/Q calcium channel activity. *FASEB J.* **15**, 1288-1290 (2001).
34. Jun,K. *et al.* Ablation of P/Q-type Ca(2+) channel currents, altered synaptic transmission, and progressive ataxia in mice lacking the alpha(1A)-subunit. *Proc. Natl. Acad. Sci. U. S. A* **96**, 15245-15250 (1999).
35. Van Den Maagdenberg,A.M. *et al.* A cacna1a knockin migraine mouse model with increased susceptibility

- to cortical spreading depression. *Neuron* **41**, 701-710 (2004).
36. Kaja, S. *et al.* Increased transmitter release at neuromuscular synapses of a novel Cacna1a S218L knock-in mouse model for familial hemiplegic migraine. *Soc. Neurosci. Abstr.* **593.4**, (2004).
 37. Maximov, A., Sudhof, T.C. & Bezprozvanny, I. Association of neuronal calcium channels with modular adaptor proteins. *J. Biol. Chem.* **274**, 24453-24456 (1999).
 38. Catterall, W.A. Interactions of presynaptic Ca²⁺ channels and snare proteins in neurotransmitter release. *Ann. N. Y. Acad. Sci.* **868**, 144-159 (1999).
 39. Lee, A. *et al.* Ca²⁺/calmodulin binds to and modulates P/Q-type calcium channels. *Nature* **399**, 155-159 (1999).
 40. Plomp, J.J. *et al.* Abnormal transmitter release at neuromuscular junctions of mice carrying the tottering alpha(1A) Ca(2+) channel mutation. *Brain* **123**, 463-471 (2000).
 41. Kaja, S. *et al.* Gene dosage-dependent transmitter release changes at neuromuscular synapses of CACNA1A R192Q knockin mice are non-progressive and do not lead to morphological changes or muscle weakness. *Neuroscience* **135**, 81-95 (2005).
 42. Yoon, C.H. Disturbances in developmental pathways leading to a neurological disorder of genetic origin, "leaner", in mice. *Dev. Biol.* **20**, 158-181 (1969).
 43. Magleby, K.L. & Stevens, C.F. A quantitative description of end-plate currents. *J. Physiol* **223**, 173-197 (1972).
 44. McLachlan, E.M. & Martin, A.R. Non-linear summation of end-plate potentials in the frog and mouse. *J. Physiol* **311**, 307-324 (1981).
 45. Eken, T. Spontaneous electromyographic activity in adult rat soleus muscle. *J. Neurophysiol.* **80**, 365-376 (1998).
 46. Giovannini, F., Sher, E., Webster, R., Boot, J. & Lang, B. Calcium channel subtypes contributing to acetylcholine release from normal, 4-aminopyridine-treated and myasthenic syndrome auto-antibodies-affected neuromuscular junctions. *Br. J. Pharmacol.* **136**, 1135-1145 (2002).
 47. Harris, J.B. & Ribchester, R.R. The relationship between end-plate size and transmitter release in normal and dystrophic muscles of the mouse. *J. Physiol* **296**, 245-265 (1979).
 48. Kuno, M., Turkanis, S.A. & Weakly, J.N. Correlation between nerve terminal size and transmitter release at the neuromuscular junction of the frog. *J. Physiol* **213**, 545-556 (1971).
 49. Lau, F.C., Abbott, L.C., Rhyu, I.J., Kim, D.S. & Chin, H.M. Expression of calcium channel alpha(1A) mRNA and protein in the leaner mouse (tg(la)/tg(la)) cerebellum. *Molecular Brain Research* **59**, 93-99 (1998).
 50. Dove, L.S., Abbott, L.C. & Griffith, W.H. Whole-cell and single-channel analysis of P-type calcium currents in cerebellar Purkinje cells of leaner mutant mice. *J. Neurosci.* **18**, 7687-7699 (1998).
 51. Wakamori, M. *et al.* Single tottering mutations responsible for the neuropathic phenotype of the P-type calcium channel. *Journal of Biological Chemistry* **273**, 34857-34867 (1998).
 52. Lambert, E.H. & Elmqvist, D. Quantal components of end-plate potentials in the myasthenic syndrome. *Ann. N. Y. Acad. Sci.* **183**, 183-199 (1971).
 53. Katz, B. & Thesleff, S. On the factors which determine the amplitude of the miniature end-plate potential. *J. Physiol.* **137**, 267-278 (1957).
 54. Plomp, J.J., van Kempen, G.T. & Molenaar, P.C. Adaptation of quantal content to decreased postsynaptic sensitivity at single endplates in alpha-bungarotoxin-treated rats. *J. Physiol* **458**, 487-499 (1992).
 55. Jen, J. *et al.* Loss-of-function EA2 mutations are associated with impaired neuromuscular transmission. *Neurology* **57**, 1843-1848 (2001).
 56. Maselli, R.A. *et al.* Presynaptic failure of neuromuscular transmission and synaptic remodeling in EA2. *Neurology* **61**, 1743-1748 (2003).
 57. Pietrobon, D. Function and dysfunction of synaptic calcium channels: insights from mouse models. *Curr. Opin. Neurobiol.* **15**, 257-265 (2005).
 58. Hu, Q., Saegusa, H., Hayashi, Y. & Tanabe, T. The carboxy-terminal tail region of human Cav2.1 (P/Q-type) channel is not an essential determinant for its subcellular localization in cultured neurones. *Genes Cells* **10**, 87-96 (2005).
 59. Sutton, K.G., McRory, J.E., Guthrie, H., Murphy, T.H. & Snutch, T.P. P/Q-type calcium channels mediate

Chapter 5

- the activity-dependent feedback of syntaxin-1A. *Nature* **401**, 800-804 (1999).
60. Jarvis, S.E., Magga, J.M., Beedle, A.M., Braun, J.E. & Zamponi, G.W. G protein modulation of N-type calcium channels is facilitated by physical interactions between syntaxin 1A and Gbetagamma. *J. Biol. Chem.* **275**, 6388-6394 (2000).
 61. Cornet, V. *et al.* Multiple determinants in voltage-dependent P/Q calcium channels control their retention in the endoplasmic reticulum. *Eur. J. Neurosci.* **16**, 883-895 (2002).
 62. Bichet, D. *et al.* The I-II loop of the Ca²⁺ channel alpha1 subunit contains an endoplasmic reticulum retention signal antagonized by the beta subunit. *Neuron* **25**, 177-190 (2000).
 63. Tottene, A., Volsen, S. & Pietrobon, D. alpha(1E) subunits form the pore of three cerebellar R-type calcium channels with different pharmacological and permeation properties. *J. Neurosci.* **20**, 171-178 (2000).
 64. Wilson, S.M. *et al.* The status of voltage-dependent calcium channels in alpha 1E knock-out mice. *J. Neurosci.* **20**, 8566-8571 (2000).
 65. Sochivko, D. *et al.* The Ca(V)2.3 Ca(2+) channel subunit contributes to R-type Ca(2+) currents in murine hippocampal and neocortical neurones. *J. Physiol* **542**, 699-710 (2002).
 66. Neelands, T.R., King, A.P. & Macdonald, R.L. Functional expression of L-, N-, P/Q-, and R-type calcium channels in the human NT2-N cell line. *J. Neurophysiol.* **84**, 2933-2944 (2000).
 67. Bourinet, E. *et al.* Interaction of SNX482 with domains III and IV inhibits activation gating of alpha(1E) (Ca(V)2.3) calcium channels. *Biophys. J.* **81**, 79-88 (2001).
 68. Arroyo, G., Aldea, M., Fuentealba, J., Albillos, A. & Garcia, A.G. SNX482 selectively blocks P/Q Ca²⁺ channels and delays the inactivation of Na⁺ channels of chromaffin cells. *Eur. J. Pharmacol.* **475**, 11-18 (2003).
 69. Newcomb, R. *et al.* Selective peptide antagonist of the class E calcium channel from the venom of the tarantula *Hysterocrates gigas*. *Biochemistry* **37**, 15353-15362 (1998).
 70. Kaja, S. *et al.* Compensatory contribution of cav2.3 channels to acetylcholine release at the neuromuscular junction of tottering mice. *J. Neurophysiol.* **95**, 2698-2704 (2006).
 71. Newcomb, R. *et al.* Selective peptide antagonist of the class E calcium channel from the venom of the tarantula *Hysterocrates gigas*. *Biochemistry* **37**, 15353-15362 (1998).
 72. Plomp, J.J., Van Den Maagdenberg, A.M., Ferrari, M.D., Frants, R.R. & Molenaar, P.C. Transmitter Release Deficits at the Neuromuscular Synapse of Mice with Mutations in the Ca(v)2.1 (alpha(1A)) Subunit of the P/Q-Type Ca(2+) Channel. *Ann. N. Y. Acad. Sci.* **998**, 29-32 (2003).